Scanning localized arc discharge lithography for the fabrication of microstructures made of carbon nanotubes

To cite this article: Y W Zhu *et al* 2007 *Nanotechnology* **18** 385304

Nanotechnology **18** (2007) 385304 (6pp) doi:10.1088/0957-4484/18/38/385304

Scanning localized arc discharge lithography for the fabrication of microstructures made of carbon nanotubes

Y W Zhu[1], C-H Sow[1,2,4], M-C Sim[1], G Sharma[3] and V Kripesh[3]

[1] Department of Physics, Faculty of Science, National University of Singapore, 2 Science Drive 3, 117542, Singapore
[2] National University of Singapore Nanoscience and Nanotechnology Initiative, 2 Science Drive 3, 117542, Singapore
[3] Institute of Microelectronics, 11 Science Park Road, Singapore Science Park II, 117685, Singapore

E-mail: physowch@nus.edu.sg

Received 11 June 2007, in final form 27 July 2007
Published 31 August 2007
Online at stacks.iop.org/Nano/18/385304

Abstract
A scanning localized arc discharge lithography (SLADL) technique has been developed in this work. The technique is based on the localized arc discharge generated between a sharp, biased conductive tip and the top surface of an oppositely biased aligned array of multi-walled carbon nanotubes (MWCNT). The arc discharge corresponds to a localized passage of electric current through the aligned array of MWCNT via the tip, which resulted in localized truncation of the MWCNT. With controlled scanning of the tip with respect to the aligned array of MWCNT, a wide variety of microstructures have been created. The morphology and the microscopic structures of the remaining MWCNT forest were investigated in detail. It was found that the passage of electric current resulted in the truncation and unraveling of the nanotubes. The SLADL represents a simple and straightforward method for the fabrication of microstructures made of carbon nanotubes.

(Some figures in this article are in colour only in the electronic version)

1. Introduction

Carbon nanotubes (CNT) are fascinating nanomaterials with unique properties that are suited for a wide variety of applications [1]. Since their discovery by Iijima [2], CNT have been utilized in nanoelectronics [3], employed in composites [4], used as electrochemical devices [5], scanning probe tips [6], field emitters [7], gas storage media [8], and etc. For the applications such as field emission, interconnect and microelectromechanical systems (MEMS), it is essential to fabricate CNT microstructures into a wide variety of patterns with specific dimensions. To create CNT microstructures, it is common to use patterned catalyst film for the control of the growth position of CNT [9], which often can be realized with various lithography routes. In addition, CNT microstructures can be created by post-growth methods such as printing, in which a solution of CNT is prepared, followed by a conventional screen printing [10], or a direct standard inkjet printer [11]. Printing typically resulted in patterns of randomly aligned CNT. Another technique to generate CNT microstructures is by way of focused laser pruning [12], in which a focused laser is utilized to locally trim away CNT for the formation of microstructures. For the ever-increasing potential applications of CNT, development of techniques for the creation of microstructures made of CNT is highly desirable. In particular, methods that are simple and economical will be attractive to researchers in this field.

In this work, we present a straightforward method for the post-processing of aligned arrays of multi-walled carbon nanotube (MWCNT) films into a wide variety of microstructures. Since the passage of sizable electric current is destructive to CNT, we can remove CNT from an aligned array of CNT forest by a high electric current. Using a sharp,

[4] Author to whom any correspondence should be addressed.

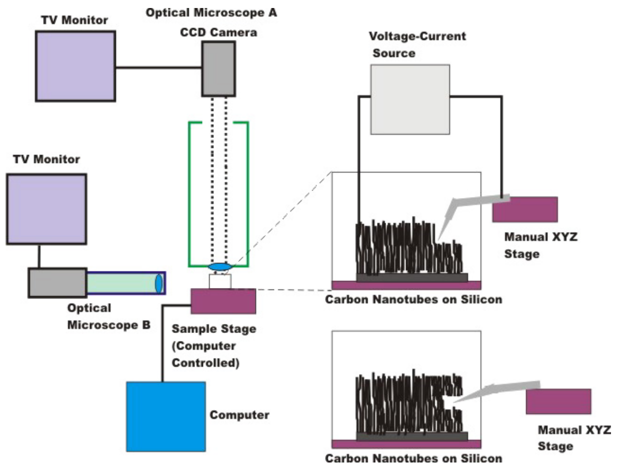

Figure 1. A schematic of the scanning localized arc discharge lithography technique. The inset shows the side cutting.

conductive and mobile needle as part of the electrical circuit, one can direct a localized flow of current at specific part of the sample. Coupled with simple scanning capability, one can create different microstructures made of CNT. Details of the effects of localized electric current on the morphological and structural changes on the CNT are investigated.

2. Experiments

Figure 1 shows a schematic set-up of the scanning localized arc discharge lithography (SLADL) technique. The main component of the experimental set-up is a sharp conductive tip, which is anchored onto a manual XYZ stage. The tungsten tip is connected to a voltage source meter, which is in turn connected to an aligned array of MWCNT grown on a Si substrate. The voltage applied varied from 20 to 80 V. The CNT were grown in a plasma enhanced chemical vapor deposition (PECVD) system, as described elsewhere [13]. As shown in figure 1, an upright optical microscope (A) was used for the top view imaging of samples. A side view of optical microscope (B) with long working distance was added to monitor and provide the side profile of the process. During the experiment, the biased tip was manually controlled to advance towards to the top surface of CNT till they touched. For the fabrication of microstructures, the MWCNT sample was positioned on a computer-controlled motorized sample stage. Motion of the MWCNT sample with respect to a stationary tip gives rise to truncated MWCNT. As-grown and as-treated samples were imaged for the morphological and structural changes by using field emission scanning electron microscopy (FESEM, JEOL 6400F), transmission electron microscopy (TEM, JEOL 3010) and Raman microscopy (Renishaw, 532 nm).

3. Results and discussion

Figure 2(a) shows a top view image of 'NUS' array from aligned MWCNT, created by the SLADL technique. Since the movement was controlled by computer program, the edge of pattern can be well defined at micrometer scale. The CNT in arc discharge treated regions were removed or partially truncated, depending on the voltage and thus the current used. During the experiment, the electric current was recorded versus time. An example of the current versus time plot at the applied voltage of 30 V is shown in figure 2(b). In figure 2(b), the peak marked I corresponds to the situation where the biased tip just touched the MWCNT sample. Destruction of the MWCNT near the tip soon after contact disconnected the electrical loop

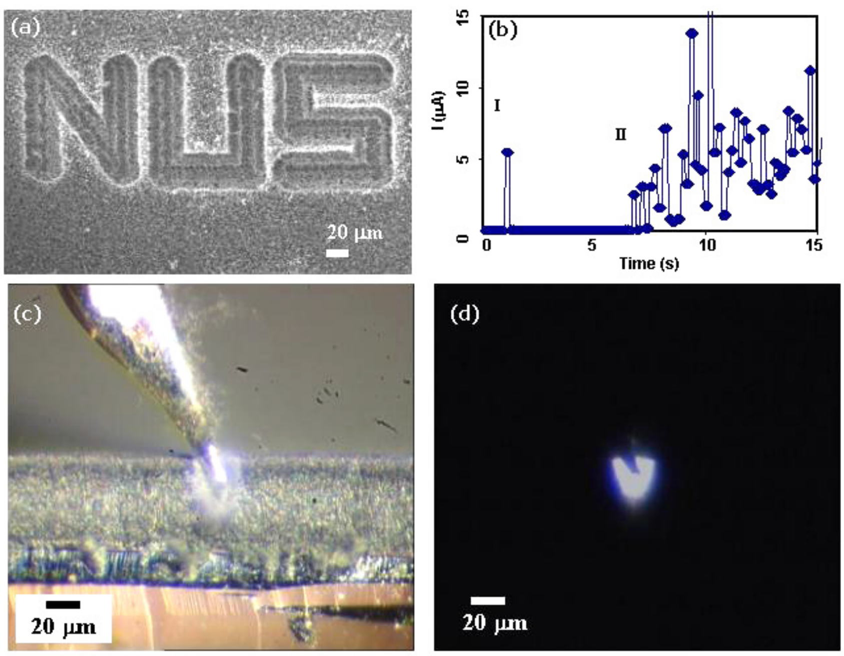

Figure 2. (a) A SEM image showing a 'NUS' pattern created by the SLADL technique; (b) an example of the measured electric current through the system versus time in a typical touch-and-scan experiment. (c) Optical micrograph of the side view of the MWCNT samples and the sharp tungsten tip. (d) Flashes of light emitted during the localized arc discharge process.

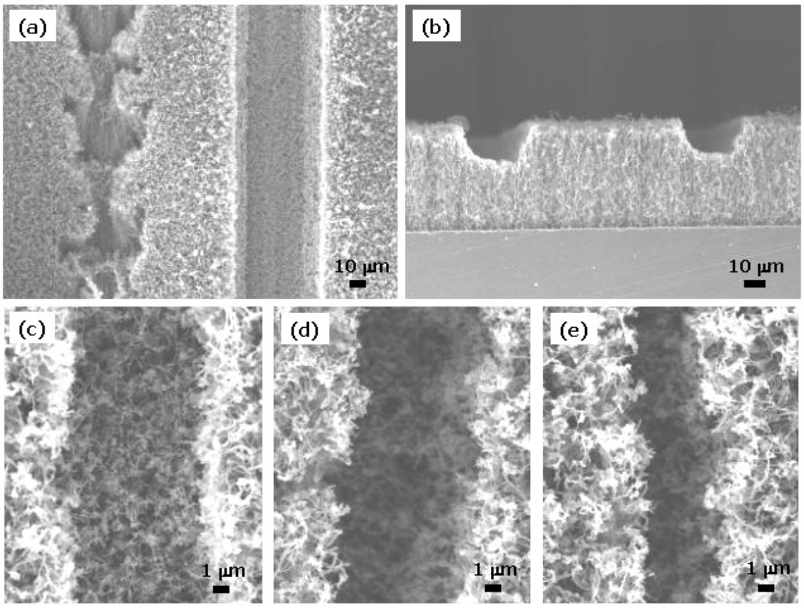

Figure 3. (a) SEM images of a needle-scratched (left) MWCNT forest and channel in the MWCNT sample created via arc discharge lithography. (b) Side view of the channels created. (c)–(e) Close-up SEM images of some of the narrow channels created by SLADL.

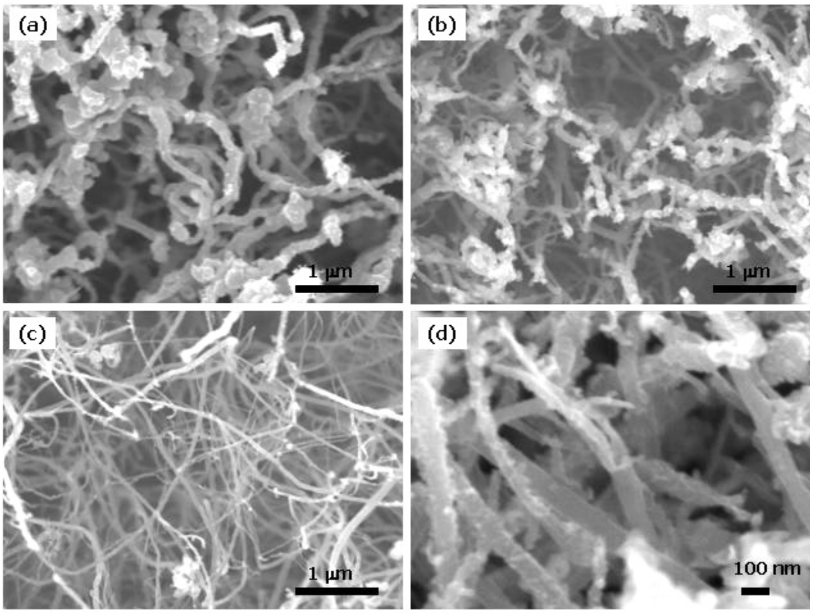

Figure 4. SEM images the morphology of (a) an as-grown MWCNT sample; MWCNT after arc discharge lithography with a bias of (b) 25 V and (c) 60 V. (d) A close-up view of a MWCNT showing some peeled portions of the nanotube.

and thus the current quickly fell back to zero. Point II in figure 2(b) corresponds to the onset of the movement of the sample stage (i.e. onset of scanning) and this provided the sustained electrical current passing through the circuit loop. The average current measured is about 5 μA. Video clips of the process of scanning localized arc discharge can be found in the supplementary materials [14]. In the experiments, we found that if the biased voltage is greater than 25 V (the value depends on the resistance of the sample), arc discharges are evidenced by bright sparks/flashes emitted at the region where the tip starts to make contact with the surface. An optical microscope image of the side view of the CNT with the scanning tip and a flash of light is shown in figure 2(c). With the illuminating light turned off, the flash of light becomes even more evident as shown in figure 2(d).

Systematic studies of the morphology and microstructures of the remaining MWCNT were carried out. Figure 3(a) shows a SEM image of a MWCNT sample comprising of two channels created without (left channel) and with (right channel) voltage bias. Obviously, it is important to apply

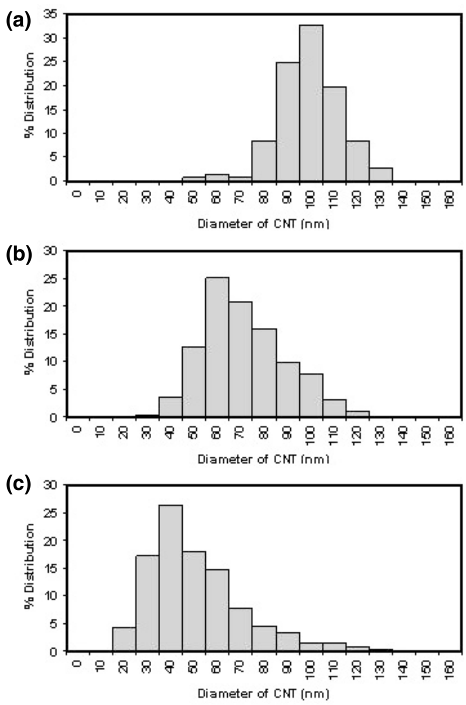

Figure 5. Measured diameter distribution of the (a) as grown MWCNT and (b) remaining MWCNT after SLADL at 25 V and (c) remaining MWCNT after SLADL at 60 V.

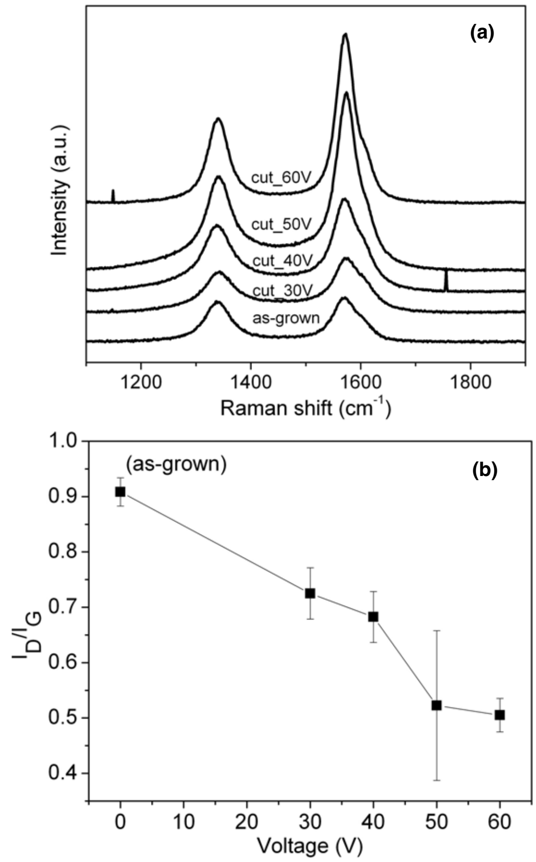

Figure 6. (a) Raman spectra of the as-grown sample and the sample after the SLADL treatment at different applied voltages. (b) I_D/I_G plot from the Raman spectra versus applied voltages.

a voltage bias between the scanning tip and the sample. Without the electrical bias, the tip would be scratching the forest of MWCNT mechanically and resulted in regions with collapsed CNT. Clearly mechanical scratching is not suitable for nanofabrication. The minimal line width (resolution) in this technique and the length of the truncated CNT depend on the voltage, shape of the tip and distance between CNT and the tip. Figure 3(b) shows the cross section of treated channels. The shape of cross section is due to the round shape of biased tips. Figures 3(c)–(e) show some of the narrow channels created using this technique.

Figures 4(a)–(c) illustrate the surface morphology of the as-grown CNT and those after exposure to the arc discharge process at a bias of 25 V and 60 V, respectively. By carefully controlling the CNT–tip distance to avoid complete removal of the CNT, some residual CNT were observed inside the channel. Notably the diameter of the MWCNT became significantly reduced after the arc discharge process. The result suggests that the passage of electric current provides sufficient energy to truncate the CNT. For the remaining MWCNT, the outer layers become unraveled, as shown in the close view image in figure 4(d). In addition, the height of remaining CNT depends on the relative distance of the scanning tip with respect to the top surface of the CNT forest. Detailed measurements of the diameter distribution of the MWCNT from the SEM images have been carried out on as-grown and SLADL treated samples. The results are shown in figure 5. The average diameter of the MWCNT reduced from 94 ± 13 nm (as-grown) to 66 ± 18 nm (after SLADL @25 V) and 45 ± 20 nm (after SLADL @60 V).

To investigate the structural changes induced by the SLADL treatment, Raman spectroscopy studies of the sample after SLADL with different voltages were carried out, as shown in figure 6(a). We can see that, after treatment the positions of D and G bands remain unchanged. However, the treated samples show a very significant reduction in the height of the peak for the D band versus the G band as shown in figure 6(b). The I_D/I_G ratio gradually reduces from 0.9 to 0.5 after arc discharge treatment at 60 V. Since D band is generally associated with the structural disorder in the nanotubes, SLADL helps to lower the degree of structural disorder in the sample.

For a better insight of the microscopic structures of the MWCNT after the localized arc discharge process, we carried out TEM imaging of MWCNT samples. To ensure that we are imaging MWCNT that have been exposed to the arc discharge process, the SLADL was carried out at a fixed voltage biased across the entire sample with a typical size of 5 mm $\times$ 5 mm. The samples were then ultrasonically dispersed in alcohol and dropped onto a TEM Cu grid for TEM/HRTEM imaging. Figure 7(a) shows a typical TEM image of as-grown MWCNT from our PECVD growth. Usually the as-grown CNT have close ends with catalyst particles inside the cap. Figures 7(b) and (c) show the HRTEM images of CNT after exposure to the arc discharge at a biased voltage of 60 V. It can be seen that the cap of some CNT has been opened (figure 7(b), dashed lines) and broken graphite layers were often found on the tip of the CNT. In addition, peeling off of the outmost layers of CNT were observed, as shown in figure 7(c), marked by an arrow.

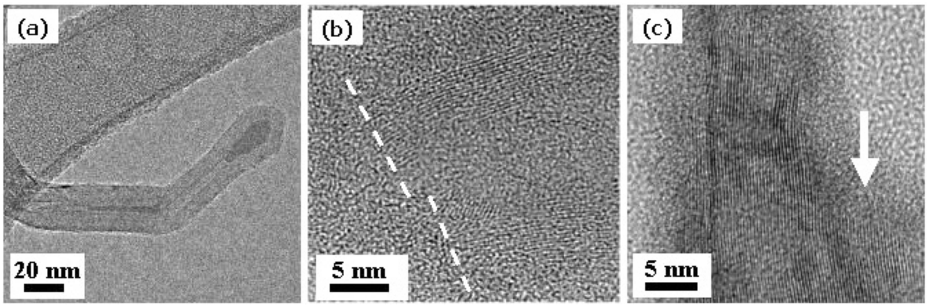

Figure 7. TEM images of (a) an as-grown MWCNT and (b), (c) MWCNT after arc discharge lithography treatment at a biased voltage of 60 V.

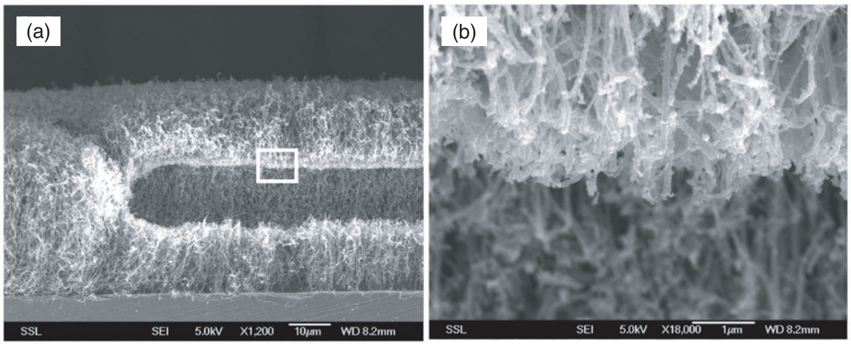

Figure 8. SEM images of the aligned MWCNT array after the sideways SLADL process.

We propose the following mechanism for the truncation of MWCNT and the observed reduction of the diameter of the MWCNT during the SLADL. The arc discharge process corresponds to the passage of large electric current through the MWCNT samples. MWCNT are conductive [15] and it has been reported that majority of the electric current passes through the outer layer of the CNT [16]. It has been reported by Smalley *et al* that applications of electric current can cause the removal of outer layer of the MWCNT [17]. Also, arc discharge has been used to open or cut isolated CNT for their length control [18]. On the other hand, a layer-by-layer destruction of a single MWCNT under a bias has been reported by Avouris *et al* [19]. Although it has been demonstrated that a MWCNT can sustain a current density larger than 10^7 A m^{-2} under a condition of ballistic transport [16], the high density of defects and large number of layers in our MWCNT make this almost impossible. Hence, at large applied current the outermost layer of the MWCNT cannot sustain the high current pulse and this results in the preferential truncation or removal of the outermost layer of CNT. And this process is accompanied with flashes as observed in our experiment and the flashes are also reported in the phenomenon during the unraveling of the CNT [17].

To further demonstrate the flexibility of the SLADL technique, a side cutting of aligned MWCNT as indicted in the schematic in figure 1 was conducted. The sharp tip readily cut away part of the cylindrical body of the MWCNT and left behind two separated segments of the CNT. SEM images of the resultant sample are shown in figure 8. Notably the segments above remained structurally stable due to the entanglement and van der Waals force among the intertwined MWCNT. A close-up view in figure 8(b) shows that treated CNT have the similar morphologies with those after top view SLADL. Combining with the side cutting, one can readily create three-dimensional microstructures based on MWCNT forests with this technique.

4. Conclusion

In conclusion, a scanning localized arc discharge lithography technique has been presented for fabricating microstructures based on MWCNT. It was found that an arc discharge generated between the top surface of biased MWCNT forests and a reversely biased tungsten tip truncated or peeled off the outmost layers of CNT. The morphological and structural changes of the remaining CNT after exposure to arc discharge have been investigated. As a simple and straightforward technique, the SLADL can be used to make a wide range of CNT-based microstructures and to control the length and diameter of MWCNT, which will find important applications in future CNT-based nanodevices and nanointerconnects.

Acknowledgments

The authors acknowledge the support from the Agency for Science Technology and Research, Singapore, under the Thematic Research Program. Y W Zhu thanks Mr B H Liu for help with the TEM study.

References

[1] Dresselhaus M S, Dresselhaus G and Avouris Ph 2001 *Carbon Nanotubes* (Berlin: Springer)

[2] Iijima S 1991 *Nature* **354** 56
[3] Avouris Ph 2002 *Chem. Phys.* **281** 429
[4] Ajayan P M, Stephan O, Colliex C and Trauth D 1994 *Science* **265** 1212
[5] An K H, Kim W S, Park Y S, Moon J M, Bae D J, Lim S C, Lee Y S and Lee Y H 2001 *Adv. Funct. Mater.* **11** 387
[6] Dai H, Hafner J H, Rinzler A G, Colbert D T and Smalley R E 1996 *Nature* **384** 147
[7] de Heer W A, Chatelain A and Ugarte D 1995 *Science* **270** 1179
[8] Dillon A C, Jones K M, Bekkedahl T A, Kang C H, Bethune D S and Heben M J 1997 *Nature* **386** 377
[9] Fan S S, Chapline M G, Franklin N R, Tombler T W, Cassell A M and Dai H 1999 *Science* **283** 512
[10] Lee N S *et al* 2001 *Diamond Relat. Mater.* **10** 265
[11] Kordas K, Mustonen T, Toth G, Jantunen H, Lajunen M, Soldano C, Talapatra S, Kar S, Vajtai R and Ajayan P M 2006 *Small* **2** 1021
[12] Lim K Y, Sow C H, Lin J, Cheong F C, Shen Z X, Thong J T L, Chin K C and Wee A T S 2003 *Adv. Mater.* **15** 300
[13] Wang Y H, Lin J, Huan C H A and Chen G S 2001 *Appl. Phys. Lett.* **79** 680
[14] Supplementary website: http://www.physics.nus.edu.sg/~physowch/SLADL/sladl.html
[15] Avouris Ph, Hertel T, Martel R, Schmidt T, Shea H R and Walkup R E 1999 *Appl. Surf. Sci.* **141** 201
[16] Frank S, Poncharal P, Wang Z L and de Heer W A 1998 *Science* **280** 1744
[17] Rinzler A G, Hafner J H, Nikolaev P, Lou L, Kim S G, Tomanek D, Nordlander P, Colbert D T and Smalley R E 1995 *Science* **269** 1550
[18] Xu Z, Dong S and Song B 2004 *CN Patent Specification* 1554578
[19] Collins P G, Hersam M, Arnold M, Martel R and Avouris Ph 2001 *Phys. Rev. Lett.* **86** 3128
Collins P G, Arnold M S and Avouris Ph 2001 *Science* **292** 706